Mon. Not. R. Astron. Soc. **393,** 527–530 (2009) doi:10.1111/j.1365-2966.2008.14160.x

Hard X-ray observations of PSR J1833−1034 and its associated pulsar wind nebula

A. De Rosa,[1⋆] P. Ubertini,[1] R. Campana,[2] A. Bazzano,[1] A. J. Dean[3] and L. Bassani[4]

[1] *INAF/IASF-Roma, Via del Fosso del Cavaliere, I-00133 Roma, Italy*
[2] *Departement of Physics, University of Rome 'La Sapienza', Piazzale A. Moro2, I-00185, Roma, Italy*
[3] *School of Physics and Astronomy, University of Southampton Highfield, Southampton*
[4] *INAF/IASF-Bologna, via Gobetti 101, I-40129 Bologna, Italy*

Accepted 2008 October 28. Received 2008 September 27; in original form 2008 September 22

ABSTRACT

PSR J1833−1034 and its associated pulsar wind nebula (PWN) have been investigated in depth through X-ray observations ranging from 0.1 to 200 keV. The low-energy X-ray data from *Chandra* reveal a complex morphology that is characterized by a bright central plerion, no thermal shell and an extended diffuse halo. The spectral emission from the central plerion softens with radial distance from the pulsar, with the spectral index ranging from $\Gamma = 1.61$ in the central region to $\Gamma = 2.36$ at the edge of the PWN. At higher energy, *INTEGRAL* detected the source in the 17–200 keV range. The data analysis clearly shows that the main contribution to the spectral emission in the hard X-ray energy range is originated from the PWN, while the pulsar is dominant above 200 keV. Recent High Energy Stereoscopic System (HESS) observations in the high-energy gamma-ray domain show that PSR J1833−1034 is a bright TeV emitter, with a flux corresponding to ∼2 per cent of the Crab in 1–10 TeV range. In addition, the spectral shape in the TeV energy region matches well with that in the hard X-rays observed by *INTEGRAL*. Based on these findings, we conclude that the emission from the pulsar and its associated PWN can be described in a scenario where hard X-rays are produced through synchrotron light of electrons with Lorentz factor $\gamma \sim 10^9$ in a magnetic field of ∼10 μG. In this hypothesis, the TeV emission is due to inverse-Compton interaction of the cooled electrons off the cosmic microwave background photons. Search for PSR J1833−1034 X-ray pulsed emission, via *RXTE* and *Swift* X-ray observations, resulted in an upper limit that is about 50 per cent.

Key words: pulsars: individual: PSR J1833−1034 – supernovae: individual: G21.5−0.9.

1 INTRODUCTION

G21.5−0.9 is a Crab nebula like supernova remnant (SNR) with a plerionic structure, i.e. with a filled centre form and a flat radio spectrum $F_\nu \propto \nu^\alpha$ with α between 0 and −0.3 (Weiler & Panagia 1978). It does not display any clear evidence of a thermal shell. Through radio observations, the system was found to include a 61.8 ms pulsar near to the centre of the nebula (Camilo et al. 2006). The X-ray morphology investigated in depth through several *Chandra* observations (Safi-Harb et al. 2001; Matheson & Safi-Harb 2005; Camilo et al. 2006) shows a near-spherical structure with a bright compact source surrounded by the PWN (∼40 arcsec in radius), which is in turn surrounded by a non-thermal halo of about 150 arcsec in radius. This extended halo shows evidence of a possible SNR structure, exhibiting filamentary-like features and limb brightening. However, the X-ray spectral emission from this region is decidedly non-thermal in character, as are the brighter knots within its envelope. The origin of this component is still unclear, but its non-thermal nature suggests that it is an extension of the synchrotron nebula (Safi-Harb et al. 2001), with a contribution of dust-scattered X-rays from the plerion (Bocchino et al. 2005). The detailed X-ray *Chandra* image of the central zone shows that the compact source, i.e. the site of the pulsar, is surrounded by a double-lobed elliptical emission region of size $\sim 7 \times 5$ arcsec^2 (Camilo et al. 2006). The offset of the pulsar from the geometrical centre of the G21.5−0.9 shell is $\lesssim$5 arcsec. The elliptical geometry is possibly an indicator of a toroidal structure around the pulsar as observed for the Crab and Vela pulsars or eventually the putative axisymmetric jet structures observed by Fürst et al. (1988) by means of high-resolution 22.3-GHz observations of this system.

The X-ray emission, as observed by *Chandra*, is well described by a power-law model with a spectral index that is a function of the angular distance from the central region (Safi-Harb et al. 2001). The point-like X-ray source within a 1-arcsec region at the site of the pulsar has a spectral index of $\Gamma = 1.4$. The spectral emission

⋆E-mail: alessandra.derosa@iasf-roma.inaf.it

from the central plerion softens with the radial distance from the pulsar, and shows a spectral index ranging from a value $\Gamma = 1.61$, in a region within the central 5 arcsec, to $\Gamma = 2.36$, at the edge. In the 0.1–10 keV energy range, the outer halo emission is generally well described by a softer spectrum with $\Gamma \sim 2.4$, while the knots have spectral indices in the range from $\Gamma \sim 2.14$ to $\sim$2.5. In 0.5–10 keV energy range, the total unabsorbed flux from the extended component and compact core is 1.1×10^{-10} erg cm^{-2} s^{-1} and the corresponding $N_{\rm H}$ value is 2.24×10^{22} cm^{-2}. Following the detailed discussion presented in Camilo et al. (2006), we adopt a distance estimate of 4.7 ± 0.4 kpc.

Careful searches in the *Chandra* and XMM data have failed to reveal any pulsed X-ray emission at the period and ephemeris of the radio pulses. La Palombara & Mereghetti (2002) set an upper limit on the 0.5 to 10 keV pulsed fraction between 7.5 and 40 per cent; however, they did not search pulsed events in the range of frequencies that comprises the spin frequency predicted by the radio ephemeris (the pulsed emission was discovered three years later by Camilo and co-workers). With a period of 61.8 ms and a period derivative of 2.02×10^{-13} s s^{-1}, the characteristic spin-down age for a braking index of $n = 3$ is 4.8 ky. PWN evolution in the light of the spinning neutron star energy-loss rate suggests that the age should be much less than 5 ky (Chevalier 2004). There is good historical evidence from ancient Chinese records to believe that PSR J1833−1034 is associated with a guest star supernova explosion that took place in BC 48, making the system just over 2050 year old (Wang, Li & Zhao 2006). This younger age implies that the pulsar was born with a period close to 47 ms.

Finally, very recently, HESS telescope has detected very high energy (VHE) emission in the TeV energy range from PSR J1833−1034 and its associated PWN (Djannati-Atai et al. 2007).

In this paper, we present the analysis of the *INTEGRAL*-IBIS (Ubertini et al. 2003) hard X-ray observation of PSR J1833−1034. The spectral information about this pulsar and its associated PWN above 10 keV was up to now still missing. To search for X-ray pulsation, we performed a detailed temporal analysis of the available archival *RXTE* and *Swift*-XRT data. In Section 2, we investigate the hard X-ray energy spectrum of the pulsar and PWN through *INTEGRAL* observation, while the TeV HESS emission from PSR J1833−1034 and its association with the hard X-ray counterpart are discussed in Section 3. Timing analysis is presented in Section 4 and finally our conclusions are drawn in Section 5.

2 THE HARD X-RAY SPECTRA OF THE PULSAR AND PWN OBSERVED BY INTEGRAL

PSR J1833−1034 has been observed as part of the third *INTEGRAL* IBIS/ISGRI (hereafter *INTEGRAL*) survey processing (Bird et al. 2007), which consists of all exposures from the beginning of the mission (2002 November) to 2006 April. The total exposure on PSR J1833−1034 is of $\sim$1.7 Ms. *INTEGRAL* images for each available pointing were generated in various energy bands using the ISDC offline scientific analysis (OSA) software (Goldwurm et al. 2003) version 5.2. The individual images were then combined to produce a mosaic of the entire sky to enhance the detection significance using the system described in detail by Bird et al. (2007). Fig. 1 shows the 17–40 keV energy-band image of the region surrounding PSR J1833−1034, and a clear excess is detected at a significance of $\sim 25\sigma$. The *INTEGRAL* image is consistent with a point-like source that is coincident with the site of PSR J1833−1034. The data are well fitted by a simple power law with photon index $\Gamma = 2.2^{+0.1}_{-0.1}$ (the spectrum is shown in the inset in Fig. 1). The 20–100 keV flux of 5.2×10^{-11} erg cm^{-2} s^{-1}, as measured by *INTEGRAL*, comprises 0.4 per cent of the pulsar spin-down luminosity of $\dot{E} = 3.38 \times 10^{37}$erg s^{-1}, assuming a distance to the source of 4.7 kpc. The most likely site of this emission should be from the central bright plerion. *Chandra* observations in 0.1–10 keV energy range have clearly detected the softening of the X-ray emission with radial distance from the pulsar, that is presumably the source of energetic electrons. This evidence has all the hallmarks of synchrotron cooling, so that we would expect the hard X-rays as observed by *INTEGRAL* to originate nearby the central source.

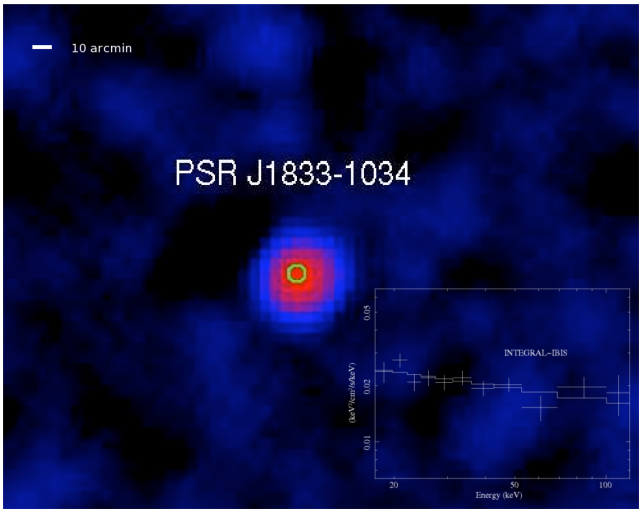

Figure 1. *INTEGRAL* image of PSR J1833−1034 in 17–40 keV range. The spatial extension of the excess reveals a point-like source. The circle represents the extension of HESS J1833−1034 (5-arcmin radius). In the inset, we show the *INTEGRAL* spectrum.

To evaluate the contribution to the *INTEGRAL* spectrum of the different components of the source (pulsar, PWN and extended emission), we plot in Fig. 2 for each component the spectral model as observed by *Chandra* (Safi-Harb et al. 2001). The low surface brightness extended emission (originated between 50- and 150-arcsec radius around the pulsar) is reproduced with a soft power law ($\Gamma = 2.36$, dashed line). The emission of the pulsar (dot–dashed curve), extracted from the central innermost region in a circle with 1-arcsec radius, is reproduced with a hard power law ($\Gamma = 1.4$). The emission of the PWN (dotted line) is extracted from a circle of 40-arcsec radius and is best fitted by a softer power law with respect to the pulsar ($\Gamma = 2.3$). All components are absorbed by a cold gas with column density $N_{\rm H} = 2.2 \times 10^{22}$ cm^{-2} as derived through *Chandra* (Safi-Harb et al. 2001) and *XMM–Newton* (Warwick et al. 2001) observations. In Fig. 2, the *INTEGRAL* data are also shown. From this figure, it appears that the pulsar contributes very little in the 20–200 keV energy range, and the extended emission is too weak with respect to the other components to affect the high-energy emission as detected by *INTEGRAL*. Therefore, the PWN is likely to contribute most to the hard X-ray flux. Indeed, the contribution of the pulsar at the 20–100 keV flux, as derived through *INTEGRAL* data, is lower than 20 per cent and it becomes even lower in the soft X-ray energy range, i.e. $\sim$3 per cent (see also Kargaltsev & Pavlov 2008). This is clearly visible in the spectral energy distribution (SED) plotted in Fig. 2. In 20–100 keV energy range, a fraction of the total emission that is larger than 80 per cent is originated in the PWN. Using the pulsar spin-down luminosity of $\dot{E} = 3.38 \times 10^{37}$erg s^{-1}, the total energy conversion efficiency (in 20–100 keV energy range) is $\eta_{\rm tot} = L_{\rm tot}/\dot{E} \sim 0.4$ per cent,

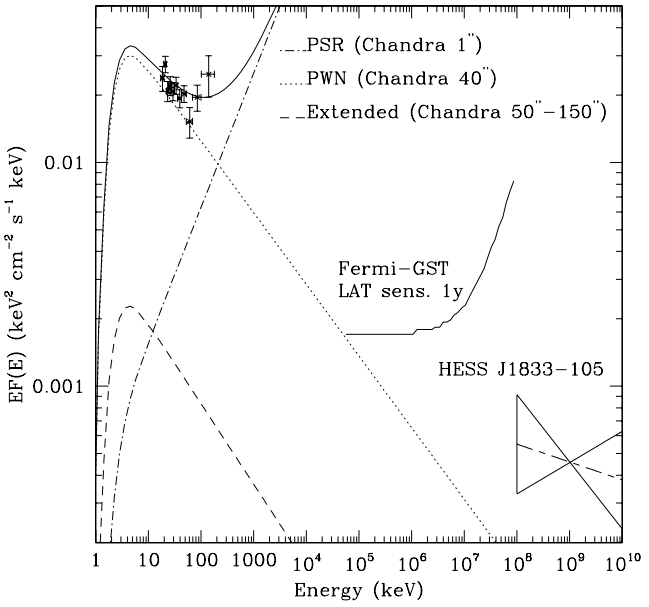

Figure 2. Spectral energy distribution from soft X-ray to TeV energy range. Each spectral component identified through *Chandra* observation has been plotted separately. *INTEGRAL* data are plotted on the top of the model. We also plot the Fermi-GST (formerly GLAST) LAT 1-year sensitivity curve taking into account the diffuse Galactic and the residual instrumental background.

with the PWN contribution that is $L_{\rm PWN}/\dot{E} \sim 0.3$ per cent and the pulsar $L_{\rm pulsar}/\dot{E} \sim 0.1$ per cent. The value of the total energy conversion efficiency $\eta_{\rm tot}$ is well in agreement with the average value measured in the others pulsar/PWM systems observed by *INTEGRAL*, that is around 1 per cent (PSR J1846−0258; McBride et al. 2008, PSR J1617−5055; Landi et al. 2007, Vela; Hoffmann, Horns & Santangelo 2007, PSR J1513−5906; Forot et al. 2006, PSR J1811−1925; Dean et al. 2008). PSR B0540−69 (Campana et al. 2008) is characterized by the highest value $\eta_{\rm tot} \sim 5.8$ per cent, while Vela by the lowest $\eta_{\rm tot} \sim 0.02$ per cent. Finally, we note that the ratio between the energy conversion efficiency of the PWN and pulsar is $\eta_{\rm PWN}/\eta_{\rm PSR} \sim 4.3$, in very good agreement with the mean value (∼4) for a sample of X-ray pulsar/PWN systems observed in the soft X-ray energy range with *Chandra* (Kargaltsev & Pavlov 2008).

3 ASSOCIATION WITH HESS J1833−105

Observations in the TeV energy range have demonstrated that PSR J1833−1034 and its associated PWN are powerful emitters in the VHE gamma-rays (Djannati-Atai et al. 2007). The position of HESS J1833−105 ($18^{\rm h}33^{\rm m}32\overset{\rm s}{.}5 \pm 0\overset{\rm s}{.}9$, $-10^{d}33\arcmin19\arcsec \pm 55\arcsec$) is in very good agreement with the location of the source detected by *INTEGRAL*. The properties of the hard X/gamma-ray emission from the pulsar/PWN system observed by *INTEGRAL* and HESS are reported in Table 1, while in Fig. 1 the HESS position is shown as a circle on the *INTEGRAL* image. The photon index of the TeV spectrum is 2.1 ± 0.2 with a flux corresponding to ∼2 per cent of the Crab (see Table 1). In Fig. 2, we report the best-fitting power law reproducing the spectrum of HESS J1833−105, with the three lines representing the upper, lower and best-fitting value of the slope. The shape of this emission, extrapolated in the X-ray energy range, matches well with the PWN spectrum observed by *INTEGRAL*, with the ratio between the X-ray and gamma-ray luminosity of $L_{\rm X}/L_\gamma \sim 30$. We assume that the soft gamma-ray emission is produced through synchrotron process of electrons in a magnetic field of 10 μG. The value of the magnetic field is close to that implied from gamma-ray observations assuming (i) the gamma-ray flux is produced by inverse-Compton (IC) scattering on cosmic microwave background (CMB) photons and (ii) a ratio $L_{\rm X}/L_\gamma \sim 30$ (Djannati-Atai et al. 2007). The equipartition value suggests the presence of a magnetic field much higher, of about $B = 0.3$ mG (Camilo et al. 2006). However, HESS observations seem to suggest that the magnetic field in PWN can be much lower than the equipartition value (Chevalier 2004). To produce the observed 20–100 keV emission through synchrotron light in 10 μG magnetic field, we need electrons with Lorentz factor of $\sim 10^9$. This value remains still very high even if we assume a higher magnetic field, e.g. $\gamma \sim 10^8$ for $B = 50$ μG. In this scenario, TeV emission can be produced through IC scattering of the same electrons population with CMB light. For electrons with Lorentz factor of $\sim 10^9$, the maximum energy gained in a single scattering is $\nu_{\rm max} = \gamma^2 \nu_{\rm CMB} \sim 10^{14}$ eV. The energy of the electrons producing TeV emission can be lower with respect to that required to produce the 20–100 keV spectrum. This matches well with the hypothesis that the TeV emission is produced by the electrons cooled through synchrotron radiation in a 10 μG field.

Future Fermi-GST observations will allow a detailed study of the SED in the MeV–GeV energy range, where the pulsar contribution should be dominant. The 1-year LAT sensitivity curve is also plotted in Fig. 2.

In the sample of pulsar/PWN systems detected by *INTEGRAL*, PSR J1833−1034 together with Crab and PSR J1846−0258 is characterized by a high $L_{20-100\,\rm keV}/L_{1-10\,\rm TeV}$ ratio and by positional coincidence with HESS. This high ratio seems to be an artefact of young pulsar/PWN systems for which the TeV source is coincident with the pulsar, and may be due to the fact that the electrons (synchrotron cooled) reservoir is not completely filled because of the lack of accumulation time.

4 TIMING ANALYSIS

In the case of *INTEGRAL* data, the combination of the cumulative long observation period and the relatively low statistical significance of the detection makes impossible to isolate and measure a pulsed hard X-ray component in the emitted flux. We then performed a period search using *RXTE*/PCA data in order to establish an upper limit on the pulsed emission in the range 2–10 keV. PSR

Table 1. Hard X/gamma-ray properties of PSR J1833−1034 and its PWN detected by *INTEGRAL* and HESS.

$F_{20-100\,\rm keV}$ (10^{-11} erg cm^{-2} s^{-1})	$^\star L_{\rm X}$(per cent $\dot{E}$) (10^{34} erg s^{-1})	$\Gamma_{\rm X}$	$F_{\rm PWN}/F_{\rm PSR}$ at 10 keV	$^\dagger L_\gamma$(per cent $\dot{E}$) (10^{34} erg s^{-1})	Γ_γ	$L_{\rm X}/L_\gamma$
5.2	13(0.4)	2.2 ± 0.1	10	0.4(0.013)	2.1 ± 0.2	30

* In 20–100 keV.
† In 1–10 TeV.

J1833−1034 has been observed once by *RXTE*, during proposal ID 20259 performed in 1997 November 8 with G21.5−0.9 as a target. We have selected PCA Good-Xenon observations, i.e. the data mode with the full-timing resolution. The data were filtered using the standard criteria (elevation angle, south atlantic anomaly passages, etc.); the baricentrization was performed using the task FXBARY and the pulsar location from *Chandra* (Camilo et al. 2006). The total exposure time on the source was 73 ks. We performed a period search in a reasonably large frequency range around the extrapolation of the radio ephemeris to the *RXTE* observation time, since the radio ephemeris were not available at the time of *RXTE* observations. We used the Z^2_m test (Buccheri et al. 1983) with $m = 2$ and 10 harmonics. We ignored the Z^2_m test with $m = 1$ because this is very powerful for sinusoidal peaks, while we have no idea on the light curve expected in our case (Protheroe 1987). We found no pulsation at the 99 per cent confidence level. Upper limits on the pulsed emission were derived with the hypothesis that the pulse shape is either sinusoidal or very narrow (in the limit of a Dirac delta shape), following the prescriptions of Protheroe (1987) and De Jager, Swanepoel & Raubenheimer (1989). For the 2–10 keV band, we obtained a flux value between 2.5 and 1.2×10^{-5} photons $\mathrm{cm^{-2}\,s^{-1}}$ for a sinusoid and a Dirac delta pulse, respectively. This pulsed flux upper limit corresponds to 1.7×10^{-13} and 8.8×10^{-14} erg $\mathrm{cm^{-2}\,s^{-1}}$, respectively, assuming that the pulsar photon index is $\Gamma = 1.5$ as found by *Chandra*. These upper limits are of the same order of magnitude, if not slightly more stringent, than those set by *Chandra* (Camilo et al. 2006). The pulsed emission is therefore lower than 50 per cent of the total emission from the pulsar.

We also analysed observations of PSR J1833−1034 made with the XRT telescope onboard the *Swift* satellite (Gehrels et al. 2004). We selected all the observations having this source in the field of view and performed in the Windowed Timing (WT) mode, that ensures the full-timing capability of this instrument, with a time resolution of about 1.7 ms. The data set contains nine pointings, performed between 2007 October 2 and 21. The total net exposure time after the standard pipeline filtering is about 52 ks. We performed a period search using an approach similar to the one used for *RXTE* observation, and still no significant pulsation was found at the 99 per cent confidence level. The upper limit on the pulsed flux was of $\sim 5 \times 10^{-13}$ erg $\mathrm{cm^{-2}\,s^{-1}}$.

5 CONCLUSIONS

The combined spectral study of the Crab-like pulsar PSR J1833−1034 and its associated PWN, over the *Chandra* and *INTEGRAL* energy range, strongly suggests that the 20–100 keV flux is mainly due to the PWN component (more than 80 per cent of the total flux), and the PSR contribution can only be dominant above 200 keV. PSR J1833−1034 is also a bright TeV emitter as detected by HESS. The *INTEGRAL* emission represents the hard X-ray counterpart to the VHE HESS source and the TeV emission matches well with the 17–200 keV spectral shape. But for PSR J1617−5055 and PSR J1513−5906, most of the pulsar/PWN systems observed by *INTEGRAL* have the hard X-ray emission dominated by the PWN. However, a detailed comparison between these sources shows that the relative contribution from the pulsar and the PWN differs very much from source to source. The observed properties of PSR J1833−1034 suggest that the hard X-ray emission is produced through synchrotron light of electrons with $\gamma \sim 10^9$ in a magnetic field of $\sim$10 μG while the TeV emission is due to IC of the cooled electrons on the CMB photons.

We note that, in the sample of pulsar/PWN systems observed by *INTEGRAL*, PSR J1833−1034 together with Crab and IGR J1846−0258 is the only system showing similar properties, i.e. high $L_{20-100\,\mathrm{keV}}/L_{1-10\,\mathrm{TeV}}$ ratio ($\gg$1) and with the position of the HESS coincident with that of the pulsar/PWN. This evidence suggests that the cooled electrons responsible for the TeV emission remain confined in the same region of the synchrotron emission. This could be an artefact of the young pulsar/PWN system.

We did not detect any evidence of pulsations in *RXTE* and *Swift*-XRT data (with upper limit for the pulsed emission of 50 per cent of the total). The lack of X-ray pulsed emission is not fully unexpected in view of the moderate magnetic field of the pulsar, $B = 3.58 \times 10^{12}$ G. However, we stress also that Crab and PSR B0540−69, clearly exhibiting X-ray pulsations, are characterized by a magnetic fields of 3.78×10^{12} and 4.96×10^{12} G, respectively, i.e. values similar to that observed in PSR J1833−1034. The lack of X-ray pulsed emission from PSR J1833−1034 could also be explained with the radio and X-ray beams pointing to different directions or with a different aperture, and the line of sight sweeps only one of them. A similar hypothesis has been proposed to explain the behaviour of Geminga and the radio-quiet pulsars (Harding, Grenier & Gonthier 2007).

ACKNOWLEDGMENTS

This program is funded by Italian Space Agency grant via contracts I/008/07/0 and I/088/06/0.

REFERENCES

Bird A. J. et al., 2007, ApJS, 170, 175
Bocchino F., van der Swaluw E., Chevalier R., Bandiera A., 2005, A&A, 442, 539
Buccheri R. et al., 1983, A&A, 128, 245
Camilo F., Ransom S. M., Gaensler B. M., Slane P. O., Lorimer D. R., Reynolds J., Manchester R. N., Murray S. S., 2006, ApJ, 637, 456
Campana R., Mineo T., De Rosa A., Massaro E., Dean A. J., Bassani L., 2008, MNRAS, 389, 691
Chevalier R. A., 2004, Adv. Space. Res, 33, 456
Dean A. J. et al., 2008, MNRAS, 384, L29
De Jager O. K., Swanepoel J. W. H., Raubenheimer B. C., 1989, A&A, 221, 180
Djannati-Atai A., for HESS collaboration, 2007, Proc. 30th ICRC, Merida, Mexico, preprint (arXiv:0710.2418)
Forot M., Hermsen W., Renaud M., Laurent P., Grenier I., Goret P., Khelifi B., Kuiper L., 2006, ApJ, 651, L45
Fürst E., Handa T., Morita K., Reich P., Reich W., Sofue Y., 1988, PASJ, 40, 347
Gehrels N. et al., 2004, ApJ, 611, 1005
Goldwurm A. et al., 2003, A&A, 411, L223
Harding A. K., Grenier I. A., Gonthier P. L., 2007, Astrophys. Space Sci, 309, 221
Hoffmann A. I. D., Horns D., Santangelo A., 2007, Ap&SS, 309, 215
Kargaltsev O., Pavlov G. G., 2008, AIP Conf. Proc., 983, 171
La Palombara N., Mereghetti S., 2002, A&A, 383, 916
Landi R., De Rosa A., Dean A. J., Bassani L., Ubertini P., Bird A. J., 2007, MNRAS, 380, 926
Matheson H., Safi-Harb S., 2005, Adv. Space Res., 35, 1099
McBride V. A. et al., 2008, A&A, 477, 249
Protheroe R. J., 1987, Proc. Astron. Soc. Aust., 2, 167
Safi-Harb S., Harrus I. M., Petre R., Pavlov G. G., Koptsevich A. B., Sanwal D., 2001, ApJ, 561, 308
Ubertini P. et al., 2003, A&A, 411, L131
Wang Z., Li M., Zhao Y., 2006, Chin. J. Astron. Astrophys., 6, 625
Warwick R. S. et al., 2001, A&A, 365, L248
Weiler K. W., Panagia N., 1978, A&A, 70, 419

This paper has been typeset from a TEX/LATEX file prepared by the author.